IEEE Access
Multidisciplinary ⁝ Rapid Review ⁝ Open Access Journal

Received December 24, 2020, accepted January 8, 2021, date of publication January 18, 2021, date of current version January 26, 2021.

Digital Object Identifier 10.1109/ACCESS.2021.3052051

Transactive Energy-Based Joint Optimization of Energy and Flexible Reserve for Integrated Electric-Heat Systems

WEI ZHAO[1], (Associate Member, IEEE), HANBIN DIAO[2], PEIQIANG LI[2], XIAOXIU LV[2], ERTAO LEI[1], (Member, IEEE), ZHENYU MAO[2], AND WENQI XUE[2]

[1]Electric Power Research Institute of Guangdong Power Grid Corporation, Guangzhou 510000, China
[2]College of Electrical and Information Engineering, Hunan University, Changsha 710000, China

Corresponding author: Peiqiang Li (lpqcs@hnu.edu.cn)

This work was supported in part by the National Key Research and Development Program of China under Grant 2018YFB0905304 and Grant 2017YFB0903403, and in part by the National Natural Science Foundation of China under Grant 51677059.

ABSTRACT Implementing integrated electric-heat systems (IEHSs) with coupled power distribution networks and district heating networks is an essential means to solve current energy problems. However, prosumers with multiple energy forms coupled and renewable energy sources with natural uncertainties pose challenges to the operation of IEHSs. This paper proposes a joint energy and reserve dispatch model for IEHSs based on transactive energy, which is a coordinated combination of a bi-level Stackelberg game and two-stage robust optimization. The bi-level Stackelberg game is used to realize the equilibrium of interests among three transacting parties, namely, integrated energy service provider (IESP), multi-carrier prosumer (MCP), and load aggregator (LA). The two-stage robust optimization is employed to ensure the reliability of the system operation under renewable energy uncertainty. In the upper level of the Stackelberg game, the IESP perform pricing and reserve dispatch, while the MCP and LA maximize their benefits via energy management in the lower level. Linearization techniques are utilized to approximate the bi-level Stackelberg game model into a single-level mixed-integer linear programming problem. The converted single-level game model is subsequently regarded as the first stage, while the real-time feasibility check is regarded as the second stage to form a two-stage robust optimization model, which is solved by a modified C&CG algorithm. Case studies demonstrate that the proposed joint energy and reserve dispatch method effectively achieves economic and reliable operation.

INDEX TERMS Integrated electric-heat system, transactive energy, joint energy and reserve dispatch, Stackelberg game, two-stage robust optimization.

I. INTRODUCTION

In response to the energy crisis and environmental concerns, investigators have begun to explore integrated energy systems to facilitate energy transformation and efficiency [1]. Constructing the integrated electric-heat system (IEHS), the market energy transaction also develops, and prosumers become more and more involved. Prosumers have source and charge attributes and are susceptive to value signals. However, due to limited capacity and lower position in the system, prosumers are short of the motivation to respond to market prices, bring many problems to the optimal operation of IEHS. An adaptive energy sharing framework transactive energy (TE) [2] is employed for solving these problems. Transactive energy is a mechanism to realize system equilibrium by economic and control means. Transactive energy regulate s the prosumers through the value signals so that the resource flexibility and the ability to promote the system safety can be utilized reasonably. Consequently, it is of profound significance to study the optimal operation of IEHS supported by the transactive energy.

With the advancement of market transactions, researchers devote themselves to studying the modeling, planning, and operation of the IEHS in the market and dispose of many economic, security problems in the operation of the IEHS through centralized dispatch, market equilibrium, and other

The associate editor coordinating the review of this manuscript and approving it for publication was Huai-zhi Wang.

methods. For economic operation, reference [3] studied the market operation strategy minimizing the operation cost. Reference [4] proposed an integrated energy micro-grid system design scheme minimizing total investment. For planning, the optimal capacity of the integrated energy system was discussed in [5]. A method for integrated energy systems expansion planning using linearized load energy curves was proposed in [6]. The optimal programming model of reliability perception was proposed in [7] and [8] to design integrated energy systems. For mathematical modeling, reference [9] provided a comprehensive mathematical model and calculation method for market clearing to study the unregulated market perspective in integrated energy systems. Reference [10] improved the optimal heat flow model and optimal power flow model for market clearing. Reference [11] proposed a two-stage hybrid random information gap decision theory model for the market clearing. Reference [12] established a bi-level Stackelberg game model between energy retailers and consumers. Reference [13], [14], and [15] presented the optimization planning model of energy transactions.

In the research mentioned above, an implicit assumption is that a central organization operates the whole system. However, in current practice, the electric-heat network and prosumers are managed by different sectors and no longer accept mandatory orders. When a central organization operates the whole system, the lack of unity and coordination among multiple parties will lead to problems such as the system's uneconomic and insecure operation. Therefore, it is crucial to construct a multiple transaction parties model. In recent research, transactive energy has been utilized to develop regional energy markets and empower market participants to engage in energy markets to achieve dynamic energy balances reliably and sustainably. Some studies applied transactive energy to different organizational patterns, [16] proposed a new distributed energy cluster organization to participate in the day-ahead market. Reference [17] and [18] presented the transactive energy supported multi-micro network system organization. For the balance of supply and demand, the power balance controller was proposed to eliminate the difference between the actual energy demand and purchase in the real-time stage in [19] and [20]. For the way of information transaction, based on multi-level transaction platforms, market operators directly coordinated and controlled prosumers by providing pricing guide in [17], [21], and [22], but [18] and [23] proposed the indirect coordination strategy that operators provided intelligent contract or price to guide electricity generating and using decisions of prosumers. Simultaneously, from the role of the transacting parties to analyze the flexibility of its operation, reference [24] proposed a trading mechanism between operators and aggregators of energy allocation among prosumers. Reference [25] presented a bi-level trading model in which prosumers are the upper leaders and users are the lower followers. Reference [26] designed an agent alliance mechanism between prosumers and operators. These different types of transacting parties have solved the system problem to some extent. However, the study of the types is not comprehensive. The potential of different types of transacting parties needs to be further explored.

Most research above focuses on the system's economic operation, but the uncertainty caused by the high proportion of intermittent renewable energy cannot be ignored. In terms of this, [27], [28] considered collaborative optimization of energy and single reserve to deal with the effects of uncertainty. However, a single reserve limits the flexibility of resource allocation in multiple transacting party system. The joint energy and multiple reserve dispatch model in the IEHS proposed in this paper is a promising study.

In this paper, we establish a joint energy and reserve dispatch model of the IEHS under the transactive energy, which integrates a reserve dispatch strategy with a flexible selection of reserve resources while considering the market pricing and dispatch of the day-ahead energy market. The model combines a bi-level Stackelberg game model and a two-stage robust optimization model. The bi-level Stackelberg game model is used to explain the equilibrium of interests of each transacting party, and the two-stage robust optimization model is used to ensure the safety and reliability of the system in uncertain scenarios. For the bi-level Stackelberg game model, the upper level is the pricing and dispatch decision of the integrated energy service provider (IESP), while the lower level is the energy management of the multi-carrier prosumer (MCP) and load aggregator (LA). The KKT condition and binary expansion technology are employed in this paper to approximately transform the bi-level Stackelberg game model into a mixed-integer linear programming model. Then the mixed-integer linear programming model is deemed as the first stage model and the real-time feasibility check as the second stage to form a two-stage robust model. The modified C&CG algorithm is utilized for processing the two-stage robust optimization model. The contributions of this paper are as follows.

1)It proposes a joint energy and reserve dispatch model of the IEHS. This model is supported by transactive energy, combines a bi-level Stackelberg game model and a two-stage robust optimization model. The KKT condition, the binary expansion technology, and the modified C&CG algorithm are utilized to solve this model.

2)It establishes a center-coordinationated featured system containing three types of transacting parties: MCP, LA, and IESP.

3)It considers the flexible reserve resources, so the IEHS can be flexible in choosing reserve service among the MCP, the LA, and the power company.

The rest of this paper is organized as follows. The framework of the transactive energy system is explained in Section II. The mathematical model for energy and reserve optimization of the integrated electric-heat system is presented in Section III. The solution method of the model is proposed in Section IV. Case studies are conducted in Section V, followed by conclusions in Section VI.

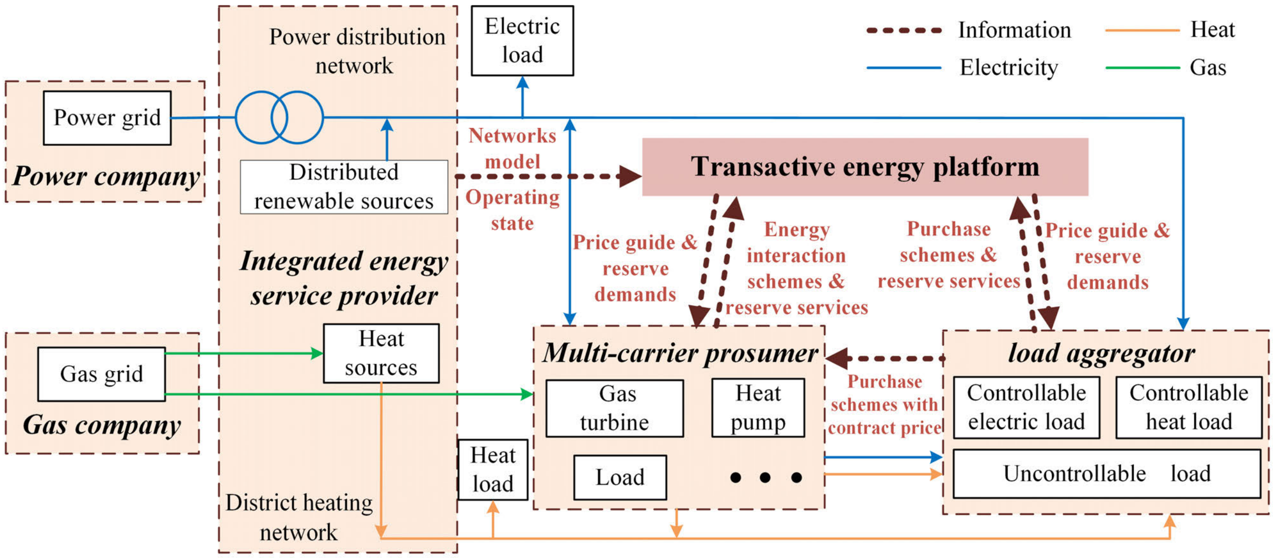

FIGURE 1. The framework of transactive energy.

II. DESCRIPTION OF TRANSACTIVE ENERGY SYSTEM

A. OPERATING FRAMEWORK

The framework of the transactive energy system proposed in this paper is shown in Figure. 1. Most of the transactive energy functions, such as the implementation of transaction processes, calculation of transaction costs, and payment of funds, are realized through the transactive energy platform. As the information transfer station of the system dispatcher, the transactive energy platform transmits information such as energy price, energy plan, and reserve capacity to the transacting parties. The primary transacted commodities on the transactive energy platform are electricity, heat, natural gas, and reserve services. The transacting parties served by the platform include an integrated energy service provider (IESP), multi-carrier prosumers (MCPs), load aggregators (LAs), power company, and gas company.

1)As the organizing entity of the IEHS, the IESP aims to meet the electric and heat needs of local consumers while minimizing economic costs. The IESP has various energy production and conversion equipment, such as distributed generation, heat pumps, and gas boilers, to service the local energy system.

2)The MCP integrates various energy production and consumption, has independent decision ability, and is sensitive to value signals. Guided by the price signal, the MCP submits power plans and reserve service to the transactive energy platform in line with its profit maximization.

3)The LA integrates multiple loads, acts as an intermediary between the IEHS and demand response resources, and takes part in the local energy market on behalf of multiple energy users. During the transactive energy operation, the LA uses demand response to minimize the energy purchase cost and takes advantage of controlling load to provide reserve service for IESP to get paid.

4)The power company benefits by selling electric power from the power grid to the IESP at the wholesale price. The gas company gets benefit by selling gas fuel from the gas grid to the IESP at the wholesale price. Besides, the IESP buys a specific reserve capacity from the power company to ensure the system is safe and reliable.

Supported by transactive energy, these transacting parties are linked together with the center-coordinationated feature. The implementation is as follows:

Firstly, the IESP transmits information such as the electric-heat networks model and operating state to the transactive energy platform used in pricing. Secondly, the MCP and the LA make their own energy plans based on the price signals of the transactive energy platform and submit transaction energy plans and reserve capacity to the transactive energy platform. Thirdly, the IESP adjusted the operating state of the IEHS according to the energy plan and reserve capacity of MCP and LA. After such multiple information transactions, the energy market completes the price clearing, and the IEHS completes the day-ahead energy and reserve dispatching. This center-coordinationated feature makes transacting parties interrelate to each other to ensure the economical and safe operation of the IEHS and enables them to make independent decisions and realize the equilibrium of interests of all transacting parties.

B. SETTINGS AND ASSUMPTIONS

Corresponding to the above operating framework of transactive energy, the settings and assumptions are made as follows.

1)The physical layer of the transactive energy system. The power distribution network (PDN) and district heating network (DHN) in IEHS are connected by the MCP, LA, and other coupling units. The power distribution network is connected to a high proportion of renewable energy. The district heating network is connected to the gas boiler, which supplies most of the heat demand as the primary heat source. The power flow state of the power distribution network is represented by the linearized branch flow model [29], the heat flow state of the district heating network is described by the thermodynamic equation of temperature control, and the energy hub (EH) [30] model is used to describe the internal energy flow state of the MCP.

2)The information layer of the transactive energy system. The operation of transactive energy needs the support of information and communication technology. It is assumed that no communication delays and packet losses when the transacting parties deliver the information through the IEP.

3)Local energy market model. The constraint relation among transacting parties is regarded as a Stackelberg game between single leader and multi-follower, and a bi-level optimization model can be established to explain it. The upper level (IESP) strategy serves as the parameter of the lower level (MCP, LA), and the lower level serves as the constraint of the upper level. The upper level can predict the response of the lower level when the lower level optimal strategy is unique. The MCP and LA take electric prices and heat prices as foregone conditions when determining energy plans, but the IESP needs to take into account the response of MCP and LA to energy prices when pricing. The equilibrium of the Stackelberg game determines the reasonable energy price and energy transaction scheme of the IEHS. In equilibrium, the interests of each transacting party are optimal, and neither party can gain profits by unilaterally changing the strategy.

4)The transaction between the MCP and LA. MCP signed the energy contract with LA, and LA buys electric energy and heat energy from MCP at the contract price. The energy transaction between MCP and LA is bound to affect the interests of IESP, so it is indispensable to study the energy transaction between MCP and LA. However, it makes the model more complex and challenging to solve. This paper assumes that the energy price of the MCP and LA transaction is a constant value and does not participate in the price clearing of the day-ahead market.

5)Reserve services. This paper focuses on the day-ahead energy and reserve dispatch and takes no account of reserve market clearing. The reserve capacity price is a definite value in our model. The reserve capacity for IEHS is provided by the MCP, LA, and power company. In view of the MCP and LA contain more flexible resources, such as cogeneration, heat pumps, and elastic loads, so the IEHS is not considered to provide the reserve services for MCP and LA.

The following describes the mathematical model and solution of the IEHS energy and reserve joint optimization supported by transactive energy in detail.

III. MATHEMATICAL FORMULATION

A. OPERATING MODEL OF MCP

From the perspective of mathematical modeling, the MCP can be regarded as an energy hub with multiple energy inputs and outputs, so we use the energy hub model to describe the energy state. Its electric energy and gas energy inputs are supplied by the power distribution network and gas company, respectively, and its electric energy and heat energy output to the IESP and LA. In addition, the gas turbine (GT) and heat pump (HP) in the MCP provide reserve capacity for the IESP.

The MCP operation model is given below. Equation (1) defines the electric power, heat energy, and gas fuel balance inside the MCP. (2) and (3) determine the equipment model of GT and HP. The reserve capacity constraints of GT and HP are limited in (4) and (5). (6) represents the reserve capacity provided by MCP to IESP.

$$P_t^{\text{I2M}} + P_t^{\text{GT}} - P_t^{\text{HP}} = P_t^{\text{M2I}} + P_t^{\text{M2L}} + P_t^{\text{MCPload}}, \quad \forall t, \tag{1a}$$

$$H_t^{\text{GTre}} + H_t^{\text{HP}} = H_t^{\text{M2I}} + H_t^{\text{M2L}} + H_t^{\text{MCPload}}, \quad \forall t, \tag{1b}$$

$$P_t^{\text{MCPgas}} = P_t^{\text{GTgas}}, \quad \forall t, \tag{1c}$$

$$P_t^{\text{GT}} = P_t^{\text{GTgas}} \eta^{\text{GT}}, \quad \forall t, \tag{2a}$$

$$H_t^{\text{GT}} = kP_t^{\text{GT}}, \quad \forall t, \tag{2b}$$

$$H_t^{\text{GT}} = H_t^{\text{GTre}} + H_t^{\text{GTdi}}, \quad \forall t, \tag{2c}$$

$$0 \le H_t^{\text{GTre}} \le \beta H_t^{\text{GT}}, \quad \forall t, \tag{2d}$$

$$H_t^{\text{HP}} = P_t^{\text{HP}} \eta^{\text{HP}}, \quad \forall t, \tag{3}$$

$$P_t^{\text{GT}} + R_t^{\text{GT+}} \le P_{\max}^{\text{GT}}, \quad \forall t, \tag{4a}$$

$$P_{\min}^{\text{GT}} \le P_t^{\text{GT}} - R_t^{\text{GT-}}, \quad \forall t, \tag{4b}$$

$$0 \le R_t^{\text{GT+}} \le R_t^{\text{up}}, \quad \forall t, \tag{4c}$$

$$0 \le R_t^{\text{GT-}} \le R_t^{\text{down}}, \quad \forall t, \tag{4d}$$

$$(P_{t-1}^{\text{GT}} + R_{t-1}^{\text{GT+}}) - (P_t^{\text{GT}} - R_t^{\text{GT-}}) \le R_t^{\text{down}}, \quad \forall t, \tag{4e}$$

$$-(P_{t-1}^{\text{GT}} - R_{t-1}^{\text{GT}-}) + (P_t^{\text{GT}} + R_t^{\text{GT+}}) \le R_t^{\text{up}}, \quad \forall t, \tag{4f}$$

$$P_t^{\text{HP}} + R_t^{\text{HP+}} \le P_{\max}^{\text{HP}}, \quad \forall t, \tag{5a}$$

$$P_{\min}^{\text{HP}} \le P_t^{\text{HP}} - R_t^{\text{HP-}}, \quad \forall t, \tag{5b}$$

$$R_t^{\text{MCP+}} = R_t^{\text{GT+}} + R_t^{\text{HP-}}, \quad \forall t, \tag{6a}$$

$$R_t^{\text{MCP}-} = R_t^{\text{GT-}} + R_t^{\text{HP+}}, \quad \forall t, \tag{6b}$$

where the superscript $X2Y$ means X to Y, representing the energy flow from X to Y, $X \in$ {IESP,MCP}, $Y \in$ {IESP,MCP,LA}, for convenience, take the first letter of X or Y; the same applies elsewhere in this paper. The decision variable P_t^{X2Y} represents the amount of electric power from X to Y at time t, H_t^{X2Y} represents the amount of heat energy from X to Y at time t. P_t^{GT}, H_t^{GT}, P_t^{HP}, H_t^{HP} are electric power and heat energy of GT and HP. P_t^{MCPload} and H_t^{MCPload} are MCP electric load and heat load. P_t^{GTgas} is the gas fuel consumed by the GT. H_t^{GTre} and H_t^{GTdi} are the recycling and discarded amount of heat energy of GT. η^{GT} is the electric efficiency of GT. η^{HP} is the heat efficiency of HP. k is the ratio of heat energy and electric power of GT. β is the discarded heat energy rate. R_t^{up} and R_t^{down} are the up and down ramp rate of the GT unit. $R_t^{\text{GT+}}/R_t^{\text{GT-}}$ and $R_t^{\text{HP+}}/R_t^{\text{HP-}}$ are the upward/downward reserve capacity of GT and HP.

In the energy transaction of the market, the objective of MCP is maximizing its interest, and the objective function is shown in equation (7). In (7), the first line is the profit of MCP from the transaction with the LA; the second line is the profit of MCP from the transaction with IESP; the third line is the reward of MCP for providing reserve service; the fourth line is the cost of MCP buying gas fuel from the gas company.

$$\begin{aligned}\max C_{\mathrm{MCP}} = \sum_t (&C_{\mathrm{e}}^{\mathrm{M2L}} P_t^{\mathrm{M2L}} + C_{\mathrm{h}}^{\mathrm{M2L}} H_t^{\mathrm{M2L}} \\ &+\psi_t^{\mathrm{M2I}} P_t^{\mathrm{M2I}} + \zeta_t^{\mathrm{M2I}} H_t^{\mathrm{M2I}} - \psi_t^{\mathrm{I2M}} P_t^{\mathrm{I2M}} \\ &+C_{\mathrm{re}}^{\mathrm{MCP}} (R_t^{\mathrm{MCP+}} + R_t^{\mathrm{MCP\text{-}}}) \\ &-C_t^{\mathrm{gas}} P_t^{\mathrm{MCPgas}}) \end{aligned} \tag{7}$$

where price variables ψ_t^{M2I}, ψ_t^{I2M}, ζ_t^{M2I}, C_t^{gas} are electric offering price, electric purchasing price, heat offering price, and gas price of MCP at time t in the day-ahead market, respectively. $C_{\mathrm{e}}^{\mathrm{M2L}}$ and $C_{\mathrm{h}}^{\mathrm{M2L}}$ are electric power and heat energy contract prices between MCP and LA. $C_{\mathrm{re}}^{\mathrm{MCP}}$ is the reserve capacity price supply for MCP.

B. OPERATING MODEL OF LA

The load types of LA are uncontrollable load and controllable load. For controllable load, we consider it the transferrable load. The operation model of LA is below. Equation (8) represents the electric power and heat energy balance. The load transfer rate is limited in (9). (10) represents LA reserve capacity constraint.

$$P_t^{\mathrm{M2L}} + P_t^{\mathrm{I2L}} = (1 - D_t^{\mathrm{Le}}) P_t^{\mathrm{LAload}}, \quad \forall t, \tag{8a}$$

$$H_t^{\mathrm{M2L}} + H_t^{\mathrm{I2L}} = (1 - D_t^{\mathrm{Lh}}) H_t^{\mathrm{LAload}}, \quad \forall t, \tag{8b}$$

$$D_{\mathrm{min}}^{\mathrm{Le}} \le D_t^{\mathrm{Le}} \le D_{\mathrm{max}}^{\mathrm{Le}}, \quad \forall t, \tag{9a}$$

$$D_{\mathrm{min}}^{\mathrm{Lh}} \le D_t^{\mathrm{Lh}} \le D_{\mathrm{max}}^{\mathrm{Lh}}, \quad \forall t, \tag{9b}$$

$$\sum_t D_t^{\mathrm{Le}} P_t^{\mathrm{LAload}} = 0, \quad \forall t, \tag{9c}$$

$$\sum_t D_t^{\mathrm{Lh}} H_t^{\mathrm{LAload}} = 0, \quad \forall t, \tag{9d}$$

$$R_t^{\mathrm{LA+}} \le (D_{\mathrm{max}}^{\mathrm{Le}} - D_t^{\mathrm{Le}}) P_t^{\mathrm{LAload}}, \quad \forall t, \tag{10a}$$

$$R_t^{\mathrm{LA\text{-}}} \le (D_t^{\mathrm{Le}} - D_{\mathrm{min}}^{\mathrm{Le}}) P_t^{\mathrm{LAload}}, \quad \forall t, \tag{10b}$$

where P_t^{I2L} and H_t^{I2L} are electric power and heat energy input to LA by IESP, respectively. P_t^{LAload} and H_t^{LAload} are the electric load and heat load in LA. D_t^{Le} and D_t^{Lh} are electric load and heat load transfer rate respectively, $D^{\mathrm{Le}}, D^{\mathrm{Lh}} \in R$, When they are positive, it means load cutting at time t, otherwise, load picking up. $R_t^{\mathrm{LA+}}$ and $R_t^{\mathrm{LA\text{-}}}$ are upward and downward reserve capacity of LA.

The objective function of LA is shown in equation (11). In (11), the first line is the cost of LA purchasing electric power and heat energy from MCP; the second line is the cost of LA purchasing electric power and heat energy from IESP; the third line is the reward of LA for providing reserve service.

$$\begin{aligned}\min C_{\mathrm{LA}} = \sum_t (&C_{\mathrm{e}}^{\mathrm{M2L}} P_t^{\mathrm{M2L}} + C_{\mathrm{h}}^{\mathrm{M2L}} H_t^{\mathrm{M2L}} \\ &+\psi_t^{\mathrm{I2L}} P_t^{\mathrm{I2L}} + \zeta_t^{\mathrm{I2L}} H_t^{\mathrm{I2L}} \\ &-C_{\mathrm{re}}^{\mathrm{LA}} (R_t^{\mathrm{LA+}} + R_t^{\mathrm{LA\text{-}}})) \end{aligned} \tag{11}$$

where P_t^{I2L} and H_t^{I2L} are the electric power and heat energy demand of LA to IESP. ψ_t^{I2L} and ζ_t^{I2L} are the electric power and heat energy purchasing price from IESP for LA. $C_{\mathrm{re}}^{\mathrm{LA}}$ is the reserve service price for LA.

C. OPERATING MODEL OF IESP

The objective of IESP is to minimize cost while the system operates safely. The revenue of IESP mainly comes from selling electric power and heat energy, and the cost mainly comes from buying electric power, heat energy, gas fuel, and reserve service. The objective function of IESP is shown in equation (12a), which is divided into two parts. The first part in (12b) represents the cost of the energy transaction, and the second part in (12c) represents the cost of reserve services.

$$\min C_{\mathrm{IESP}} = C_{\mathrm{energ}} + C_{\mathrm{re}} \tag{12a}$$

$$\begin{aligned} C_{\mathrm{energ}} = \sum_t (&\psi_t^{\mathrm{M2I}} \cdot P_t^{\mathrm{M2I}} - \psi_t^{\mathrm{I2M}} P_t^{\mathrm{I2M}} + \zeta_t^{\mathrm{M2I}} H_t^{\mathrm{M2I}} \\ &- \psi_t^{\mathrm{I2L}} P_t^{\mathrm{I2L}} + \zeta_t^{\mathrm{I2L}} H_t^{\mathrm{I2L}} + C_t^{\mathrm{gas}} P_t^{\mathrm{gas}} + C_t^{\mathrm{grid}} P_t^{\mathrm{grid}}) \end{aligned} \tag{12b}$$

$$\begin{aligned} C_{\mathrm{re}} = \sum_t (&C_{\mathrm{re}}^{\mathrm{MCP}} (R_t^{\mathrm{MCP+}} + R_t^{\mathrm{MCP\text{-}}}) \\ &+ C_{\mathrm{re}}^{\mathrm{LA}} (R_t^{\mathrm{LA+}} + R_t^{\mathrm{LA\text{-}}}) + C_{\mathrm{re}}^{\mathrm{grid}} (R_t^{\mathrm{grid+}} + R_t^{\mathrm{grid\text{-}}})) \end{aligned} \tag{12c}$$

where C_{energ} is the function of energy transaction cost. C_{re} is the cost of reserve service. P_t^{gas} is the gas fuel inflow of GB. P_t^{grid} is the amount of electric power obtained from the power company. C_t^{grid} is the electric power price provided by the power company. $C_{\mathrm{re}}^{\mathrm{grid}}$ is the reserve service price provided by the power company. $R_t^{\mathrm{grid+}}$ and $R_t^{\mathrm{grid\text{-}}}$ are the upward and downward reserve capacity of MCP.

1) NETWORK CONSTRAINS

The IEHS energy network is composed of the power distribution network and district heating network. The mathematical models of the district heating network and power distribution network are shown in equation (13) and equation (14), respectively. (13a) is the heat flow balance of node of heat pipeline, (13b) is the temperature drop of water in the pipeline. Equations (14a) and (14b) represent the balance of active and reactive power of the bus. (14c) is the voltage equation of the bus. Upper and lower voltage limits are in (14d).

$$\sum_{L:(L,i)\in Z_{\mathrm{heat}}^{\mathrm{to}}} (c_{\mathrm{w}} G_{L,t} T_{L,t}^{c}) + H_{i,t}^{\mathrm{g}} - H_{i,t}^{\mathrm{load}} = \sum_{L:(L,i)\in Z_{\mathrm{heat}}^{\mathrm{fr}}} (c_{\mathrm{w}} G_{L,t}) T_{i,t}, \quad \forall i,\ \forall t, \tag{13a}$$

$$T_{i,t} - T_{L,t}^{\mathrm{en}} = (T_{L,t}^{\mathrm{c}} - T_{L,t}^{\mathrm{en}}) e^{\frac{\lambda \sigma_L}{c_{\mathrm{w}} G_{L,t}}}, i \in Z_{\mathrm{heat}}^{\mathrm{fr}}(L), \quad \forall L,\ \forall t, \tag{13b}$$

$$T_{i,t,\mathrm{min}} \le T_{i,t} \le T_{i,t,\mathrm{max}}, \quad \forall i,\ \forall t, \tag{13c}$$

$$\sum_{l:(l,j)\in Z_{\text{ele}}^{\text{to}}} P_{l,t}^{\text{f}} + P_{j,t}^{\text{g}} - P_{j,t}^{\text{load}} = \sum_{l:(l,j)\in Z_{\text{ele}}^{\text{fr}}} P_{l,t}^{\text{f}}, \quad \forall j, \forall t, \tag{14a}$$

$$\sum_{l:(l,j)\in Z_{\text{ele}}^{\text{to}}} Q_{l,t}^{\text{f}} + Q_{j,t}^{\text{g}} - Q_{j,t}^{\text{load}} = \sum_{l:(l,j)\in Z_{\text{ele}}^{\text{fr}}} Q_{l,t}^{\text{f}}, \quad \forall j, \forall t, \tag{14b}$$

$$\sum_{j:(l,j)\in Z_{\text{ele}}^{\text{fr}}} V_{j,t} - \sum_{j:(l,j)\in Z_{\text{ele}}^{\text{to}}} V_{j,t} = \frac{r_l P_{l,t}^{\text{f}} + x_l Q_{l,t}^{\text{f}}}{V_{\text{n}}}, \quad \forall l, \forall t, \tag{14c}$$

$$V_{j,\min} \le V_{j,t} \le V_{j,\max}, \quad \forall l, \forall t, \tag{14d}$$

where i and j are the node of district heating network (DHN) and the bus of power distribution network (PDN), respectively. L and l are the pipeline in DHN and the line in PDN, respectively. $Z_{\text{heat}}^{to}/Z_{\text{heat}}^{fr}$ are the mapping of the set of pipelines into the set of pipeline outlet/inlet nodes. c_w is the specific heat capacity of water, $G_{L,t}$ is the mass flow rate of pipeline L at time t. $T_{L,t}^{c}$ is the outlet temperature of pipeline L. $T_{i,t}$ is the inlet temperature of pipeline L, and the temperature of node i. $T_{en,t}$ is the ambient temperature. $H_{i,t}^{\text{g}}$ and $H_{i,t}^{\text{load}}$ are the heat energy generation and heat load of node i at time t. λ is heat conductivity of the pipeline. σ_L is the length of the pipeline. $Z_{\text{ele}}^{to}/Z_{\text{ele}}^{fr}$ are the mapping of the set of electric lines into the set of electric line end/head buses. $P_{l,t}^{\text{f}}/Q_{l,t}^{\text{f}}$ are active/reactive power in distribution lines. $P_{j,t}^{\text{g}}/P_{j,t}^{\text{load}}$ and $Q_{j,t}^{\text{g}}/Q_{j,t}^{\text{load}}$ are active and reactive power generation/load at bus j at time t. $V_{j,t}/V_{\text{n}}$ are voltage magnitude at bus j/slack bus. r_l and x_l are line resistance and reactance.

2) TRANSACTIVE CONSTRAINS

IESP should also specify the maximum amount of energy transaction when making the energy transaction price so as to avoid the risk due to the energy transaction. Equation (15) represents the upper and lower limits of the transactive power between the electric power and heat energy.

$$0 \le P_t^{d} \le P_{t,\text{qua}}^{d}, \quad \forall d \in \{\text{I2M,M2I,I2L}\}, \quad \forall t, \tag{15a}$$

$$0 \le H_t^{d} \le H_{t,\text{qua}}^{d}, \quad \forall d \in \{\text{M2I,I2L}\}, \quad \forall t, \tag{15b}$$

where the superscript d is the direction of energy flow. It should be noted that $P_{t,\text{qua}}^{d}$ and $H_{t,\text{qua}}^{d}$ are the variables in the upper level of the IESP model. P_t^{d} and H_t^{d} are the variables in the lower level of MCP and LA models. Besides, the transaction energy between IESP and MCP needs to be constrained so that the energy purchase and sale do not exist simultaneously. The expression is shown in (16).

$$0 \le P_{\text{qua},t}^{\text{I2M}} \le MZ_t^{\text{IM}}, \quad \forall t, \tag{16a}$$

$$0 \le P_{\text{qua},t}^{\text{M2I}} \le M(1 - Z_t^{\text{IM}}), \quad \forall t, \tag{16b}$$

where Z_t^{IM} is a binary variable, When the value is 1, the energy is sold by IESP to MCP, and vice versa.

3) RESERVE CONSTRAINS

The reserve capacity for IEHS is provided by the power company in addition to the MCP and LA. Equation (17) represents the constraint of reserve capacity provided by the power company. Equation (18) indicates that MCP and LA provide reserve services according to the demands of IESP; that is, the reserve capacity provided by MCP and LA should not be more than the reserve demands of IESP.

$$P_t^{\text{grid}} + R_t^{\text{grid+}} \le P_{\max}^{\text{grid}}, \quad \forall t, \tag{17a}$$

$$P_t^{\text{grid}} - R_t^{\text{grid-}} \ge P_{\min}^{\text{grid}}, \quad \forall t, \tag{17b}$$

$$0 \le R_t^{e+} \le R_{t,\text{qua}}^{e+}, \quad \forall e \in \{\text{MCP, LA}\}, \forall t, \tag{18a}$$

$$0 \le R_t^{e-} \le R_{t,\text{qua}}^{e-}, \quad \forall e \in \{\text{MCP, LA}\}, \forall t, \tag{18b}$$

where the superscript e represents the transacting parties in the transactive energy system. It should be noted that $R_{t,\text{qua}}^{e+}$ and $R_{t,\text{qua}}^{e-}$ are reserve demand variables of the IESP model. R_t^{e+} and R_t^{e-} are reserve variables of the MCP and LA models.

D. REAL-TIME FEASIBILITY CHECK

Considering the impact of the forecast error of renewable energy on system security, the operation of IEHS based on robust optimization should have at least one feasible state in the real-time stage. Therefore, the following constraints are added to ensure the viability of IEHS operating in the real-time stage. J_{SP} is the objective function of the feasibility check problem in (19). When $J_{\text{SP}} = 0$, it means that when the uncertain parameter is set at any value within the fluctuation interval, the power deviation and voltage deviation of the system are zero; that is, the system can still operate stably in the worst scenario. Equation (20) represents the electric power balance constraint and voltage constraint with uncertain parameters added. Equation (21) is the relationship between the power adjustment amount of system flexibility resources and reserve capacity. Equation (22) is the set of uncertain parameters.

$$J_{\text{SP}} = \max_{\hat{P}_t^{\text{WT}} \in U} \min_{\substack{\Delta\hat{P}_{j,t}^{e}, \hat{s}_{j,t}^{+}, \hat{s}_{j,t}^{-} \\ \hat{V}_{j,t}^{+}, \hat{V}_{j,t}^{-}}} \sum_t \sum_j (\hat{V}_{j,t}^{+} + \hat{V}_{j,t}^{-} + \hat{s}_{j,t}^{+} + \hat{s}_{j,t}^{-}) \tag{19a}$$

$$J_{\text{SP}} = 0 \tag{19b}$$

$$\sum_{l:(l,j)\in Z_{\text{ele}}^{\text{fr}}} \hat{P}_{l,t}^{\text{f}} - \sum_{l:(l,j)\in Z_{\text{ele}}^{\text{to}}} \hat{P}_{l,t}^{\text{f}} + P_{j,t}^{\text{load}} - P_{j,t}^{\text{g}} = \Delta\hat{P}_{j,t}^{e} + \hat{P}_{j,t}^{\text{WT}} + \hat{s}_{j,t}^{+} - \hat{s}_{j,t}^{-}, \quad \forall j, \forall t, \forall l \tag{20a}$$

$$\hat{s}_{j,t}^{+}, \hat{s}_{j,t}^{-} \ge 0, \quad \forall j, \forall t, \tag{20b}$$

$$\sum_{j:(l,j)\in Z_{\text{ele}}^{\text{fr}}} \hat{V}_{j,t} - \sum_{j:(l,j)\in Z_{\text{ele}}^{\text{to}}} \hat{V}_{j,t} = \frac{r_l \hat{P}_{l,t}^{\text{f}} + x_l Q_{l,t}^{\text{f}}}{V_{\text{n}}} \quad \forall j, \forall t, \forall l, \tag{20c}$$

$$V_{\min} - \hat{V}_{j,t}^{-} \le \hat{V}_{j,t} \le V_{\max} + \hat{V}_{j,t}^{+}, \quad \forall j, \forall t, \tag{20d}$$

$$\hat{V}_{j,t}^{+}, \hat{V}_{j,t}^{-} \ge 0, \quad \forall j, \forall t, \tag{20e}$$

$$-R_{j,t}^{e-} \leq \Delta\hat{P}_{j,t}^{e} \leq R_{j,t}^{e+}, \quad \forall e \in \{\text{MCP, LA, grid}\}, \forall j, \forall t, \tag{21}$$

$$U = \{\hat{P}_t^{\text{WT}} = P_t^{\text{WT},0} + \alpha^{\text{WT}} P_t^{\text{WT},0}(z_{k,t}^{+} - z_{k,t}^{-}), \quad \forall k, \forall t, \tag{22a}$$

$$z_{k,t}^{+}, z_{k,t}^{-} \in \{0,1\}, z_{k,t}^{+} + z_{k,t}^{-} \leq 1, \quad \forall k, \forall t, \tag{22b}$$

$$\sum_t (z_{k,t}^{+} + z_{k,t}^{-}) \leq \Gamma_T, \quad \forall k, \forall t \tag{22c}$$

$$\sum_k (z_{k,t}^{+} + z_{k,t}^{-}) \leq \Gamma_K, \quad \forall k, \forall t.\} \tag{22d}$$

where $\hat{P}_t^{\text{WT}}$ is the uncertain parameter at time t, $P_t^{\text{WT},0}$ is the expected value of the uncertain parameter. U is the set of uncertainties. α^{WT} is the forecast error ratio of wind power, which can be obtained through a statistical analysis of historical data. $z_{k,t}^{+}$ and $z_{k,t}^{-}$ denote the robust adjustment coefficient of uncertain parameters. Γ_T and Γ_K are the temporal and spatial uncertainty budgets, respectively. k and K are any equipment and equipment set that bring uncertainty, respectively. $\Delta\hat{P}_{j,t}^{e}$ is the amount of power adjustment to deal with uncertainties. e is the set of the MCP, LA, and power company. $\hat{V}_{j,t}^{+}/\hat{V}_{j,t}^{-}$ and $\hat{s}_{j,t}^{+}/\hat{s}_{j,t}^{-}$ are the positive/negative slack variables of voltage and power balance constraints, respectively. $\hat{P}_{l,t}^{\text{f}}$ and $\hat{V}_{j,t}$ are the real-time stage variables, which are the active power in electric line l and the voltage of bus j.

To sum up, the IEHS energy and reserve joint optimization model established in this paper can be expressed as equation (23). The model considers the balance of interests of all parties in transactive energy and the safe operation with uncertainties.

$$\min C_{\text{IESP}}(12) \tag{23a}$$
$$\text{s.t. Network constraints}(13), (14) \tag{23b}$$
$$\text{Transactive constraints}(15), (16) \tag{23c}$$
$$\text{Reserve constraints}(17), (18) \tag{23d}$$
$$\text{MCP operation model}(1)-(7) \tag{23e}$$
$$\text{LA operation model}(8)-(11) \tag{23f}$$
$$\text{Real-time feasibility check}(19)-(22) \tag{23g}$$
$$\text{Upper and lower limits of other variables.} \tag{23h}$$

The (23) model is a nonlinear programming problem, and the nonlinearity is reflected in three main parts. Part 1, the bilinear term is composed of price variable and energy transaction variable in (23a). Part 2, the addition of (23e) and (23f) makes the model become a bi-level Stackelberg game problem. Part 3, the addition of (23g) makes the model a two-stage robust problem.

Next, we will deal with the nonlinear part of the model properly so that the model can be resolved reliably.

IV. SOLUTION METHODOLOGY

For the above nonlinear model, the solution is as follows. First, the linearization method deals with part 1 and part 2: The KKT condition is used to process the linear MCP and LA models, making the bi-level Stackelberg game a single-level model. The bilinear term in (23a) is approximately converted into a linear term using binary expansion technology. Secondly, a two-stage robust model is established, and the modified column and constraint generation (C&CG) algorithm is used to solve the model effectively. The solution method is introduced in detail below.

A. LINEARIZATION METHODOLOGY

The Stackelberg game relation of the transacting parties can be described by a bi-level model. (23a), (23b), (23c), and (23d) constitute the upper level model for decisions made by IESP, (23e) and (23f) constitute the lower level model for decisions made by MCP and LA. It should be noticed that the MCP and LA models of the lower level are linear, so the KKT condition can be used to convert the lower level model into constraints. The MCP and LA models are abstracted into the following expressions.

$$\min(\begin{bmatrix}\mathbf{c}^{\text{T}} \mathbf{y}_{\text{oob}}^{\text{T}}\end{bmatrix}\begin{bmatrix}\mathbf{x}_{\text{lir}} \\ \mathbf{x}_{\text{lre}}\end{bmatrix}) \tag{24a}$$

$$\text{s.t.} \begin{bmatrix}\mathbf{A}_1 & \mathbf{A}_2 \\ \mathbf{B}_1 & \mathbf{B}_2\end{bmatrix}\begin{bmatrix}\mathbf{x}_{\text{lir}} \\ \mathbf{x}_{\text{lre}}\end{bmatrix} \leq \begin{bmatrix}\mathbf{b} \\ \mathbf{y}_{\text{oie}}\end{bmatrix}, \tag{24b}$$

$$\begin{bmatrix}\mathbf{D}_1 & \mathbf{D}_2 \\ \mathbf{E}_1 & \mathbf{E}_2\end{bmatrix}\begin{bmatrix}\mathbf{x}_{\text{lir}} \\ \mathbf{x}_{\text{lre}}\end{bmatrix} = \begin{bmatrix}\mathbf{y}_{\text{oe}} \\ \mathbf{m}\end{bmatrix}, \tag{24c}$$

where $\mathbf{x}$ is the vector variable, represents the decision variables of the lower level model. $\mathbf{x}_{\text{lir}}/\mathbf{x}_{\text{lre}}$ are the decision variables of the lower level model that are irrelevant/related to the decision variables of the other level models, such as decision variables P_t^{I2L} and H_t^{I2L} belong to $\mathbf{x}_{\text{lre}}$ in LA model. $\mathbf{y}$ is the decision variable of other level models. $\mathbf{y}_{\text{oob}}$ is the decision variable of other level models in the objective function, such as the variables ψ_t^{M2I}, ψ_t^{I2M}, and ζ_t^{M2I} of the upper level IESP in the objective function of MCP. $\mathbf{y}_{\text{oie}}$ is the decision variable of other level models in the inequality constraint, such as decision variable $P_{t,\text{qua}}^{\text{I2M}}$ of IESP in MCP model. $\mathbf{y}_{\text{oe}}$ is the decision variable of other level models equality constraint, such as decision variables P_t^{M2L} and H_t^{M2L} of LA in MCP model.

By introducing these four sets of Lagrangian multipliers such as $\boldsymbol{\mu}_1, \boldsymbol{\mu}_2, \boldsymbol{\lambda}_1, \boldsymbol{\lambda}_2$, the Lagrangian equation is as follows:

$$\begin{aligned} L(\mathbf{x}_{\text{lir}}, \mathbf{x}_{\text{lre}}) = {} & \mathbf{c}^{\text{T}}\mathbf{x}_{\text{lir}} + \mathbf{y}_{\text{oob}}^{\text{T}}\mathbf{x}_{\text{lre}} + \boldsymbol{\mu}_1^{\text{T}}(\mathbf{A}_1\mathbf{x}_{\text{lir}} + \mathbf{A}_2\mathbf{x}_{\text{lre}} - \mathbf{b}) \\ & + \boldsymbol{\mu}_2^{\text{T}}(\mathbf{B}_1\mathbf{x}_{\text{lir}} + \mathbf{B}_2\mathbf{x}_{\text{lre}} - \mathbf{y}_{\text{oie}}) + \boldsymbol{\lambda}_1^{\text{T}}(\mathbf{D}_1\mathbf{x}_{\text{lir}} \\ & + \mathbf{D}_2\mathbf{x}_{\text{lre}} - \mathbf{y}_{\text{oe}}) \\ & + \boldsymbol{\lambda}_2^{\text{T}}(\mathbf{E}_1\mathbf{x}_{\text{lir}} + \mathbf{E}_2\mathbf{x}_{\text{lre}} - \mathbf{m}). \end{aligned} \tag{25}$$

Get the following constraints by KKT transformation:

$$\mathbf{c} + \mathbf{A}_1^{\text{T}}\boldsymbol{\mu}_1 + \mathbf{B}_1^{\text{T}}\boldsymbol{\mu}_2 + \mathbf{D}_1^{\text{T}}\boldsymbol{\lambda}_1 + \mathbf{E}_1^{\text{T}}\boldsymbol{\lambda}_2 = \mathbf{0}, \tag{26a}$$
$$\mathbf{y}_{\text{oob}} + \mathbf{A}_2^{\text{T}}\boldsymbol{\mu}_1 + \text{B}_2^{\text{T}}\boldsymbol{\mu}_2 + \mathbf{D}_2^{\text{T}}\boldsymbol{\lambda}_1 + \mathbf{E}_2^{\text{T}}\boldsymbol{\lambda}_2 = \mathbf{0}, \tag{26b}$$
$$\boldsymbol{\mu}_1^{\text{T}}(\mathbf{A}_1\mathbf{x}_{\text{lir}} + \mathbf{A}_2\mathbf{x}_{\text{lre}} - \mathbf{b}) = 0, \quad \boldsymbol{\mu}_1 \geq \mathbf{0}, \tag{26c}$$
$$\boldsymbol{\mu}_2^{\text{T}}(\mathbf{B}_1\mathbf{x}_{\text{lir}} + \mathbf{B}_2\mathbf{x}_{\text{lre}} - \mathbf{y}_{\text{oe}}) = 0, \quad \boldsymbol{\mu}_2 \geq \mathbf{0}, \tag{26d}$$
$$\text{Original constraints}(24\text{b}), (24\text{c}). \tag{26e}$$

Another difficulty is coming from the bilinear term in equation (23a), such as $\psi_t^{\mathrm{M2I}} P_t^{\mathrm{M2I}}$ and $\psi_t^{\mathrm{I2M}} P_t^{\mathrm{I2M}}$, which are described by xy. In this paper, the big-M and binary expansion technology are adopted for processing the bilinear term. Particularly, we use 2^K discrete points to approximate possible values of y in its feasible interval $\left[y^l, y^m\right]$. The approximation accuracy of binary expansion can be controlled by the number of expansion segments. After introducing the auxiliary variable v_k, the bilinear term can be expressed in the following equation (27).

$$xy = xy^l + \Delta y(2^0 v_0 + 2^1 v_1 + \cdots + 2^k v_k), \tag{27a}$$

$$v_k = xz_k, \tag{27b}$$

$$\Delta y = \frac{y^m - y^l}{2^k - 1}, \tag{27c}$$

$$x_k - M(1 - z_k) \leq v_k \leq x_k + M(1 - z_k), \quad \forall k, \tag{27d}$$

$$-Mz_k \leq v_k \leq Mz_k, \quad \forall k, \tag{27e}$$

where $k = 1, 2, 3 \ldots n$, z is a binary variable with the same dimension of x and y. As long as the M parameter is large enough, this transformation is exact, and no accuracy is lost.

B. MODIFIED C&CG ALGORITHM

After the linearization above, equation (23) becomes a two-stage robust model, equations (23a) - (23f) constitute the first stage, equation (23g) constitutes the second stage. In the optimization of the two-stage robust model, the day-ahead scheduling stage (first stage) decision results are obtained by taking the system economy as the optimization objective, and the real-time scheduling stage (second stage) decision results can be obtained based on the determined first-stage decision variables even in the worst scenario.

The proposed two-stage robust model can be described by equation (28). (28a) means to minimize the energy and reserve cost of IEHS, and the bilinear term can be linearized through (27). (28b) represents the compact form of system operation constraints in the first stage, which are corresponding equations (23e) - (23f) processed by the KKT condition and equations (23b) - (23d). Equation (28c) is the compact form of system operation constraints with uncertain parameters in the second stage, the corresponding equation (23g) specifically. Equation (28d) represents the value range of the variable, the corresponding equation (23h) specifically.

$$\min_{\mathbf{p},\mathbf{h},\mathbf{r}} \boldsymbol{\psi}^{\mathrm{T}}\mathbf{p} + \boldsymbol{\zeta}^{\mathrm{T}}\mathbf{h} + \mathbf{C}^{\mathrm{T}}\mathbf{r} \tag{28a}$$

$$\text{s.t. } \mathbf{A}^{\mathrm{T}}\mathbf{p} + \mathbf{B}^{\mathrm{T}}\mathbf{h} + \mathbf{E}^{\mathrm{T}}\mathbf{r} + \mathbf{F}^{\mathrm{T}}\mathbf{u}^0 \leq \mathbf{b}, \tag{28b}$$

$$\forall \mathbf{u} \in U, \exists \boldsymbol{\Delta} : \mathbf{G}^{\mathrm{T}}\boldsymbol{\Delta} \leq \mathbf{b} - \mathbf{F}^{\mathrm{T}}\mathbf{u} - \mathbf{A}^{\mathrm{T}}\mathbf{p} - \mathbf{B}^{\mathrm{T}}\mathbf{h} - \mathbf{E}^{\mathrm{T}}\mathbf{r}, \tag{28c}$$

$$\mathbf{p} \in P, \mathbf{h} \in H, \mathbf{r} \in R, \tag{28d}$$

where $\boldsymbol{\psi}$ and $\boldsymbol{\zeta}$ are the price vectors. $\mathbf{p}$ is the electric power vector. $\mathbf{h}$ is the heat energy vector. $\mathbf{r}$ is the reserve capacity vector. $\mathbf{u}^0$ is the expected value of wind power. $\mathbf{u}$ is the uncertain variable of wind power. $\boldsymbol{\Delta}$ is the amount of power adjustment in the real-time stage.

For the two-stage robust optimization problem, the specific steps of the modified C&CG algorithm are described as follows.

Algorithm 1 The Modified C&CG Based Solution Procedure

Initialization: set $k = 0$, $J_{\mathrm{SP}0} = +\infty$.
Repeat
➡ solve the following master problem:
MP: $\min \boldsymbol{\psi}^{\mathrm{T}}\mathbf{p} + \boldsymbol{\zeta}^{\mathrm{T}}\mathbf{h} + \mathbf{C}^{\mathrm{T}}\mathbf{r}$
s.t. $\mathbf{A}^{\mathrm{T}}\mathbf{p} + \mathbf{B}^{\mathrm{T}}\mathbf{h} + \mathbf{E}^{\mathrm{T}}\mathbf{r} \leq \mathbf{b} - \mathbf{F}^{\mathrm{T}}\mathbf{u}^0$,
$\mathbf{A}^{\mathrm{T}}\mathbf{p}+\mathbf{B}^{\mathrm{T}}\mathbf{h}+\mathbf{E}^{\mathrm{T}}\mathbf{r}+\mathbf{G}^{\mathrm{T}}\boldsymbol{\Delta}^l \leq \mathbf{b}-\mathbf{F}^{\mathrm{T}}\mathbf{u}_l^*, \forall 1 \leq l \leq k$
$\mathbf{p} \in P, \mathbf{h} \in H, \mathbf{r} \in R$
Derive an optimal solution ($[\mathbf{p}_{\mathrm{k+1}}^*, \mathbf{h}_{\mathrm{k+1}}^*, \mathbf{r}_{\mathrm{k+1}}^*, \boldsymbol{\psi}_{k+1}^*, \boldsymbol{\zeta}_{k+1}^*, \Delta^{1*}, \Delta^{2*}, \ldots, \Delta^{k*}]$).
➡ Calculate
SP: $J_{\mathrm{SP}}(\mathbf{p}_{\mathrm{k+1}}^*, \mathbf{h}_{\mathrm{k+1}}^*, \mathbf{r}_{\mathrm{k+1}}^*)$
If $J_{\mathrm{SP}}(\mathbf{p}_{\mathrm{k+1}}^*, \mathbf{h}_{\mathrm{k+1}}^*, \mathbf{r}_{\mathrm{k+1}}^*) > \varepsilon$, create variables $\boldsymbol{\Delta}^{k+1}$
and add the following constraints to MP:
$\mathbf{A}^{\mathrm{T}}\mathbf{p} + \mathbf{B}^{\mathrm{T}}\mathbf{h} + \mathbf{E}^{\mathrm{T}}\mathbf{r} + \mathbf{G}^{\mathrm{T}}\boldsymbol{\Delta}^{k+1} \leq \mathbf{b} - \mathbf{F}^{\mathrm{T}}\mathbf{u}_{k+1}^*$,
where $\mathbf{u}_{k+1}^*$ is the scenario generated from the solution for $J_{\mathrm{SP}}(\mathbf{p}_{\mathrm{k+1}}^*, \mathbf{h}_{\mathrm{k+1}}^*, \mathbf{r}_{\mathrm{k+1}}^*)$. Note that duality
is used to solve the max-min problem in this paper.
Until $J_{\mathrm{SP}} \leq \varepsilon$, return $[\mathbf{p}_{\mathrm{k+1}}^*, \mathbf{h}_{\mathrm{k+1}}^*, \mathbf{r}_{\mathrm{k+1}}^*, \boldsymbol{\psi}_{k+1}^*, \boldsymbol{\zeta}_{k+1}^*]$, and terminate.

In conclusion, the essence of the two-stage robust optimization is to decompose the energy and reserve joint optimization problem of IEHS into economic operation in the first stage and safe operation in the second stage. In the first stage (day-ahead stage), according to the Stackelberg game model converted by the KKT condition, the optimal solution of energy, price, and the reserve is solved, and the optimal solution is returned to the SP model. By solving the second stage (real-time stage) model after duality, the algorithm determines whether the solution of the first stage satisfies the power balance and voltage limitation of the system. If the power balance and voltage limits are not met, the worst scenario obtained in the second stage is returned to MP, and MP is solved again to obtain a first-stage solution. The iteration cycle of the optimized solution is not completed until a solution satisfying the requirements is found.

V. CASE STUDIES

A. BASIC CONFIGURATIONS

The system consists of a modified IEEE 33-bus power distribution network (PDN) and a 32-node district thermal network (DHN) [13]. The prosumer connects to the PDN at Bus 12 and the DHN at Node 31. The load aggregator connects to the PDN at Bus 29 and the DHN at Node 1. Two wind turbines are connected to the PDN Bus 13 and Bus 28, respectively. The system topology is shown in Figure 2. The parameters of the prosumer and the DHN are shown in Tables 1 and 2, respectively, and the bounds of other

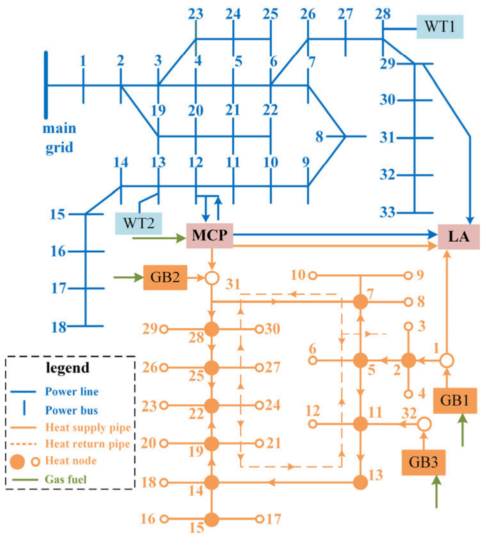

FIGURE 2. The topology of the system.

TABLE 1. Parameters of the MCP.

	Power limit (MW)	Efficiency	Heat - electric ratio	Range of ramp rate (MW/h)	Range of discarded heat rate
GT	[0.4,4]	0.4	1.5	[-0.65, 0.65]	[0, 20%]
HP	[0,0.25]	-	3	-	-

TABLE 2. Parameters of the heat sources in DHN.

	Node	Capacity (MW)	Efficiency	Unit cost of production $/(MWh)
GB1	1	3	1	20
GB2	31	2	1	20
GB3	32	2	1	20

TABLE 3. Bounds of other variables.

Variable	Interval	Variable	Interval
V	[0.93, 1.07] p.u.	D^{Le}	[-20%, 20%]
T (supply pipeline)	[70, 100] ℃	D^{Lh}	[-20%, 20%]
T (return pipeline)	[35, 65] ℃	$R^{\mathrm{grid+,-}}$	[0, 1] MW

variables are shown in Table 3. The electric load, heat load, and the forecasts for wind turbines are shown in Figure 3. The flexible electric load controllable periods of the load aggregator are 3, 7, and 20, and the flexible thermal load controllable periods are 1, 15, and 17. The electric price in the wholesale electric market, the gas price in the wholesale gas market, and the contract price signed between the MCP and the LA are shown in Figure 4. The prices for the prosumer, the load aggregator, and the main grid to provide reserve ancillary services are taken as 70, 50, and 80$/MW, respectively.

In our checks, 128 discrete points (K = 7) are used for the binary expansion scheme. All the simulations are written in YALMIP by calling Gurobi on a computer with 2.6 GHz and 8 GB RAM.

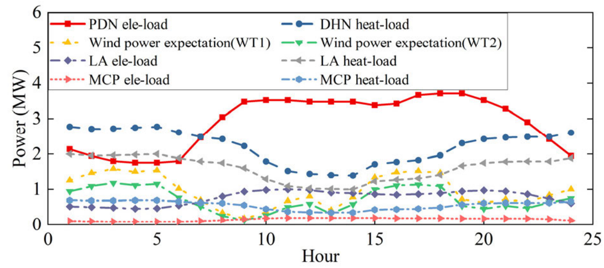

FIGURE 3. Electric load, heat load and wind power forecast profiles.

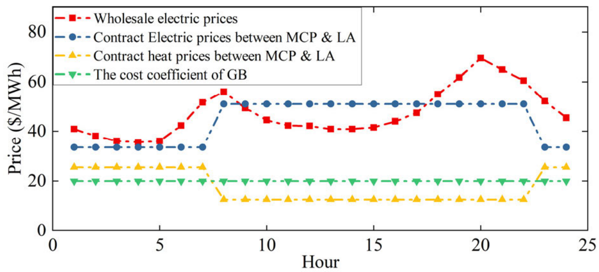

FIGURE 4. The known price curves.

1) Set different forecast error ratios of wind power. By setting different wind power forecast error ratios, we can get different reserve capacity dispatch conditions. Here, we set the forecast error ratios α^{WT} as 5%, 10%, 15%, 20% and 25% orderly. The temporal uncertainty budget Γ_T takes 24, and the spatial uncertainty budget Γ_K takes 2. The forecast error ratio for the benchmark case takes 15%.

2)Set different contract prices. The electric and heat contract prices between the MCP and the LA vary proportionally. The contract prices are multiplied by the same variation factor $\alpha_{contract}$, which increases from 0.2 to 3 orderly. The variation factor $\alpha_{contract}$ of the benchmark scenario is 1.

3)Set different optimization models. We build the deterministic energy and reserve optimization model (shortened to DM) and the conventional energy and reserve optimization model (shortened to CM), respectively, and compare these two models with the model proposed in this paper. The DM does not consider the real-time feasibility check, and the following equation (29) limit its reserve capacity:

$$R_t^{\mathrm{GT+}} + R_t^{\mathrm{HP-}} + R_t^{\mathrm{LA+}} + R_t^{\mathrm{grid+}} \geq 0.15 P_t^{\mathrm{WT,0}}, \quad \forall t, \quad (29a)$$
$$R_t^{\mathrm{GT-}} + R_t^{\mathrm{HP+}} + R_t^{\mathrm{LA-}} + R_t^{\mathrm{grid-}} \geq 0.15 P_t^{\mathrm{WT,0}}, \quad \forall t, \quad (29b)$$

The CM is divided into two separate models that are the day-ahead energy optimization and reserve optimization. The model of the CM does not consider the influence of reserve dispatching on the day-ahead energy market. The model firstly conducts the pricing and dispatch of the day-ahead energy market without considering the uncertainty of renewable energy to obtain the day-ahead energy market operation results and then conducts two-stage robust optimization of the reserve capacity based on the operation results of the day-ahead energy market so as to obtain the reserve results.

B. RESULTS

1) THE BENCHMARK CASE

The electric and heat prices, the transactive electric power, and heat energy of the IEHS are shown in Figures 5, 6, 7, and 8. If the price of a certain period is 0, it means no energy transaction.

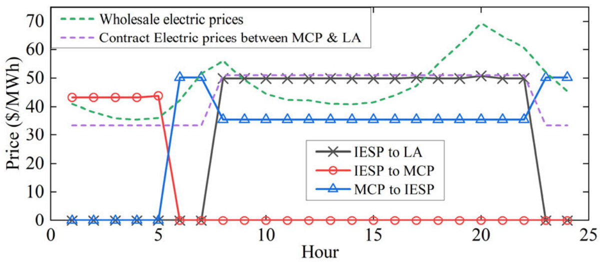

FIGURE 5. Electric price results for the benchmark case.

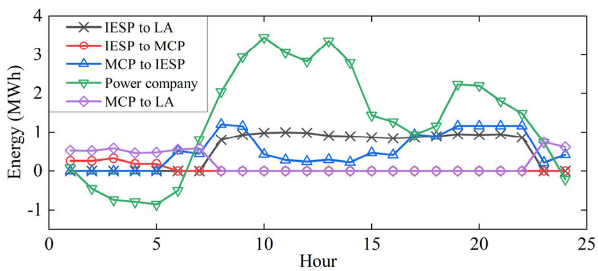

FIGURE 6. Electric power transaction results for the benchmark case.

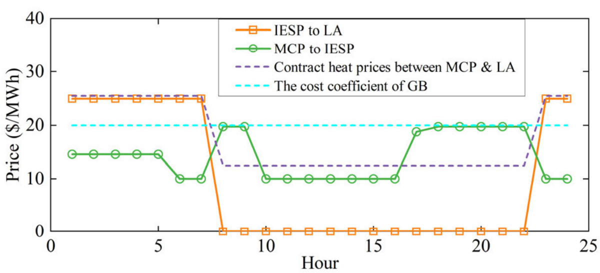

FIGURE 7. Heat price results for the benchmark case.

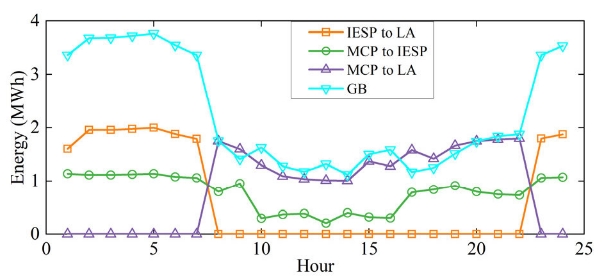

FIGURE 8. Heat energy transaction results for the benchmark case.

In periods 1-5, the electric price provided by the IESP to the MCP is higher than the price in the wholesale electric market, and the IESP sells electric power to the MCP to increase its revenue. In periods 7-23, the electric price purchased by the IESP from the MCP is lower than the price in the wholesale electric market, and the IESP reduces its own cost of electric purchase by purchasing electric power from the MCP.

From the perspective of the LA, in periods 1-7, the heat energy price sold by the IESP is lower than the heat contract price of the MCP, so the LA chooses to purchase heat energy from the IESP instead of the MCP, thus reducing its own heat purchasing cost. In periods 8-22, the electric price sold by the IESP is lower than the electric contract price sold by the MCP, so the LA chooses to purchase electric power from the IESP, thus reducing its cost of electric power purchasing.

From the perspective of the MCP, in periods 1-5, the MCP purchases a certain amount of electric power from the IESP at 43$/MWh, which is mainly used for heat pump heat production, while the MCP sell the produced heat to the IESP at the price of 14.5$/MWh. The calculation based on the heat pump efficiency ($\eta^{\mathrm{HP}} = 3$) shows that the MCP can make some profits by producing heat efficiently through the heat pump and using the price difference between the electric power and heat energy for arbitrage.

Thus, it is known that the IEHS supported by the transactive energy uses the value to ensure that transacting parties are profitable and to motivate them to participate in the optimal operation of the IEHS effectively.

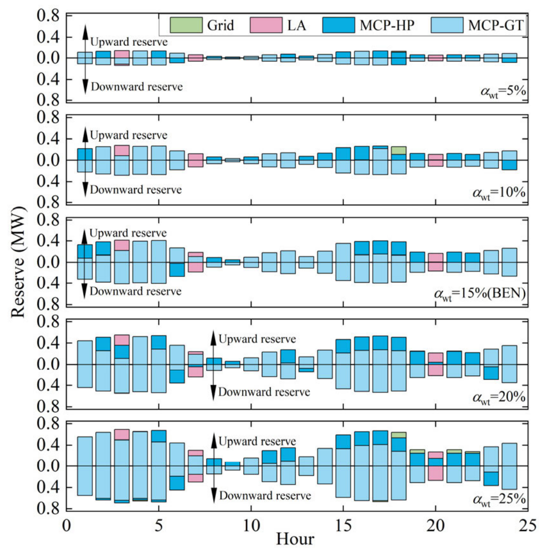

FIGURE 9. Reserve dispatch results under different wind power forecast errors.

2) IMPACT OF WIND POWER FORECAST ERRORS

The reserve dispatching of the IEHS for different wind power different forecast error ratios is shown in Figure 9. Due to the lower cost of the IESP to purchase reserve capacity from MCP and LA, most of the reserve capacity is provided by MCP and LA. During periods of high wind power expectations, for example, in periods 0-5 and 15-18, the IEHS requires more reserve capacity. In periods of low wind power expectation, for example, in periods 7-10, the IEHS requires less reserve capacity. It shows that the wind power expectation level affects the amount of reserve capacity. The reserve dispatch is not only related to wind power expectations but also related to the wind power forecast error ratio range. As the wind power forecast error ratio increases, more reserve capacity is required for the IEHS.

TABLE 4. Cost of IESP and run time under different contract prices.

$\alpha_{contract}$	Energy transaction cost ($)					Reserve cost ($)	Total Cost ($)	Time (s)
	Cost			Revenue				
	Grid	Gas	MCP	MCP	LA			
0.2	1190	853	535	41	**0**	831	**3368**	23
0.6	1189	848	540	35	**7**	831	**3366**	27
1(BEN)	1584	1083	754	30	**1106**	828	**3114**	310
1.4	1638	1102	780	0	**1599**	828	**2749**	463
1.8	1612	1214	943	0	**1921**	832	**2680**	470
2.2	1673	1387	946	12	**2277**	830	**2548**	578
2.6	1722	1415	904	7	**2382**	829	**2481**	615
3	1722	1415	905	8	**2382**	829	**2481**	608

3) IMPACT OF CONTRACT PRICE

Since the energy purchase strategy of the LA is related to the offered electric and heat energy prices of IESP and MCP, the contract prices between MCP and LA will have an impact on the revenue of the IESP. The operating costs of the IESP and run time in different contract prices are shown in Table 4. It is clear that when contract prices between the MCP and the LA are meager, the LA hardly buys energy from the IESP, and the total cost of the IESP is the highest at this time. As contract prices increase, the LA gradually purchases electric power and heat energy from the IESP, and the total cost of the IESP decreases. When contract prices increase to a certain value, the revenue of the IESP from the LA is stable at $2382, and the total cost of the IESP is stable at $2481. Thus, the contract prices between MCP and LA affect the share of energy supplied by the IESP to the LA, which affects the total cost of the IESP in turn. The higher the contract price is, the more revenue the IESP receives from the LA, and the lower the total cost of the IESP is. We should also note that the change in the contract price also affects the solution time of the model.

4) COMPARISON OF DIFFERENT MODELS

We analyze the operation risk of the model proposed in this paper, the DM and the CM. First, 100 possible actual wind power scenarios are obtained by random sampling. Then, based on the sampled wind power scenarios, the real-time feasibility checks are performed according to the above three optimization results, and the values of the objective function J_{sp} are calculated and shown in Figure 10. It indicates that the real-time scheduling stage cannot meet the security operation requirements when the value of J_{sp} is more than 0. As we can see from Figure 10, the proposed model in this paper and the CM meet the security operation requirements in each scenario, while the DM fails to meet the security operation requirements in some scenarios.

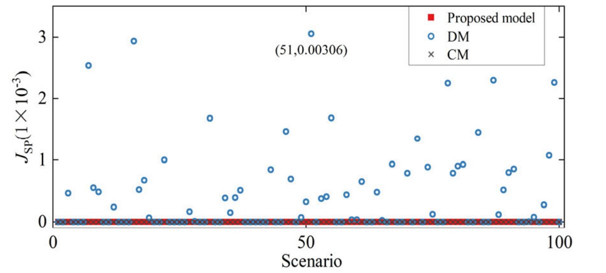

FIGURE 10. Real-time feasibility check results.

In scenario 51, although the operation strategy obtained by the DM can meet the real-time power balance constraint, the voltage magnitude of PDN buses 31-33 is lower than 0.93 at period 13. It is because that the DM does not consider the redistribution of power flow after power adjustment. So, even though the reserve capacity is numerically sufficient, the DM cannot guarantee the security of the dispatch strategy and cannot satisfy the voltage constraint in the real-time stage. The model proposed in this paper and the CM can realize the security operation of the IEHS.

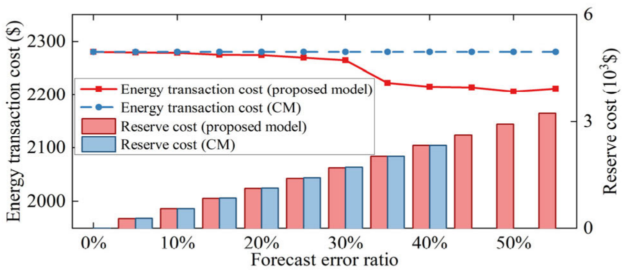

FIGURE 11. Comparison of energy transaction cost and reserve cost results of the proposed model and the CM under different wind power forecast error ratios.

By varying the forecast error ratio, the costs of energy transaction and reserve of the model proposed and the CM are shown in Figure 11. When the forecast error of wind power is small, there is almost no difference between the energy transaction cost and reserve cost of IEHS of the two models. However, when the forecast error ratio of wind power is large (the forecast error ratio is more than 30%), the energy transaction cost of the proposed model decreases to a certain extent. It is because that the proposed model optimizes the energy and reserve joint dispatching of the IEHS, which improves the economy of operation. When the forecast error ratio of wind power increase to more than 45%, the reserve dispatching of the CM becomes unsolvable, while the proposed model can still solve the reserve results. Therefore, the model proposed in this paper is more advantageous to the security and reliability of IEHS operation with the condition of high uncertainties.

VI. CONCLUSION

This study proposes a joint energy and reserve dispatch model for an IEHS under transactive energy, with a modified

C&CG algorithm and linearization techniques such as the KKT condition and the binary expansion method to solve it. In the proposed transactive energy system framework with center-coordinationated feature, each transacting party is motivated to participate in supply and demand balancing and optimal dispatch proactively. Case studies show that the multi-carrier prosumer utilizes its energy conversion equipment and energy prices at different periods to achieve arbitrage. The load aggregator flexibly chooses energy suppliers and energy purchase periods to reduce costs. The IESP could flexibly select reserve resources, such as reserve services from multi-carrier prosumers and load aggregators. Besides, the transaction price between the multi-carrier prosumer and the load aggregator could affect the share of energy supplied by the IEHS to the load aggregator, which affects the economic benefits of the IESP. The proposed method achieves economic operation of the IEHS by using price signals to guide the energy management of multi-carrier prosumer and load aggregator, as well as guarantees high reliability of the system under uncertain operating conditions through reserve dispatch and robust optimization.

REFERENCES

[1] D. Xu, B. Zhou, Q. Wu, C. Y. Chung, C. Li, S. Huang, and S. Chen, "Integrated modelling and enhanced utilization of power-to-ammonia for high renewable penetrated multi-energy systems," *IEEE Trans. Power Syst.*, vol. 35, no. 6, pp. 4769–4780, Nov. 2020, doi: 10.1109/TPWRS.2020.2989533.

[2] T. Pinto, R. Faia, M. A. F. Ghazvini, J. Soares, J. M. Corchado, and Z. Vale, "Decision support for small players negotiations under a transactive energy framework," *IEEE Trans. Power Syst.*, vol. 34, no. 5, pp. 4015–4023, Sep. 2019, doi: 10.1109/TPWRS.2018.2861325.

[3] J. Hu, G. Yang, H. W. Bindner, and Y. Xue, "Application of network-constrained transactive control to electric vehicle charging for secure grid operation," *IEEE Trans. Sustain. Energy*, vol. 8, no. 2, pp. 505–515, Apr. 2017, doi: 10.1109/TSTE.2016.2608840.

[4] A. K. Bejestani, A. Annaswamy, and T. Samad, "A hierarchical transactive control architecture for renewables integration in smart grids: Analytical modeling and stability," *IEEE Trans. Smart Grid*, vol. 5, no. 4, pp. 2054–2065, Jul. 2014, doi: 10.1109/TSG.2014.2325575.

[5] Y. Wang, Z. Huang, Z. Li, X. Wu, L. Lei Lai, and F. Xu, "Transactive energy trading in reconfigurable multi-carrier energy systems," *J. Mod. Power Syst. Clean Energy*, vol. 8, no. 1, pp. 67–76, 2020, doi: 10.35833/MPCE.2018.000832.

[6] Z. Yang, J. Hu, X. Ai, J. Wu, and G. Yang, "Transactive energy supported economic operation for multi-energy complementary microgrids," *IEEE Trans. Smart Grid*, vol. 12, no. 1, pp. 4–17, Jan. 2021, doi: 10.1109/TSG.2020.3009670.

[7] Z. Liu, L. Wang, and L. Ma, "A transactive energy framework for coordinated energy management of networked microgrids with distributionally robust optimization," *IEEE Trans. Power Syst.*, vol. 35, no. 1, pp. 395–404, Jan. 2020, doi: 10.1109/TPWRS.2019.2933180.

[8] A. Arabkoohsar and G. B. Andresen, "Dynamic energy, exergy and market modeling of a high temperature heat and power storage system," *Energy*, vol. 126, pp. 430–443, May 2017.

[9] V. Davatgaran, M. Saniei, and S. S. Mortazavi, "Optimal bidding strategy for an energy hub in energy market," *Energy*, vol. 148, pp. 482–493, Apr. 2018.

[10] K. Bruninx, H. Pandzic, H. Le Cadre, and E. Delarue, "On the interaction between aggregators, electricity markets and residential demand response providers," *IEEE Trans. Power Syst.*, vol. 35, no. 2, pp. 840–853, Mar. 2020, doi: 10.1109/TPWRS.2019.2943670.

[11] S. Khazeni, A. Sheikhi, M. Rayati, S. Soleymani, and A. M. Ranjbar, "Retail market equilibrium in multicarrier energy systems: A game theoretical approach," *IEEE Syst. J.*, vol. 13, no. 1, pp. 738–747, Mar. 2019.

[12] Y. Cao, W. Wei, L. Wu, S. Mei, M. Shahidehpour, and Z. Li, "Decentralized operation of interdependent power distribution network and district heating network: A market-driven approach," *IEEE Trans. Smart Grid*, vol. 10, no. 5, pp. 5374–5385, Sep. 2019, doi: 10.1109/TSG.2018.2880909.

[13] R. Li, W. Wei, S. Mei, Q. Hu, and Q. Wu, "Participation of an energy hub in electricity and heat distribution markets: An MPEC approach," *IEEE Trans. Smart Grid*, vol. 10, no. 4, pp. 3641–3653, Jul. 2019.

[14] M. A. Mirzaei, M. Nazari-Heris, B. Mohammadi-Ivatloo, K. Zare, M. Marzband, M. Shafie-Khah, A. Anvari-Moghaddam, and J. P. S. Catalao, "Network-constrained joint energy and flexible ramping reserve market clearing of power- and heat-based energy systems: A two-stage hybrid IGDT–stochastic framework," *IEEE Syst. J.*, early access, Jun. 8, 2020, doi: 10.1109/JSYST.2020.2996952.

[15] D. Xu, B. Zhou, K. W. Chan, C. Li, Q. Wu, B. Chen, and S. Xia, "Distributed multienergy coordination of multimicrogrids with biogas-solar-wind renewables," *IEEE Trans. Ind. Informat.*, vol. 15, no. 6, pp. 3254–3266, Jun. 2019, doi: 10.1109/TII.2018.2877143.

[16] W. Liu, J. Zhan, C. Y. Chung, and Y. Li, "Day-ahead optimal operation for multi-energy residential systems with renewables," *IEEE Trans. Sustain. Energy*, vol. 10, no. 4, pp. 1927–1938, Oct. 2019, doi: 10.1109/TSTE.2018.2876387.

[17] Y. Li, Y. Zou, Y. Tan, Y. Cao, X. Liu, M. Shahidehpour, S. Tian, and F. Bu, "Optimal stochastic operation of integrated low-carbon electric power, natural gas, and heat delivery system," *IEEE Trans. Sustain. Energy*, vol. 9, no. 1, pp. 273–283, Jan. 2018, doi: 10.1109/TSTE.2017.2728098.

[18] F. Lezama, J. Soares, P. Hernandez-Leal, M. Kaisers, T. Pinto, and Z. Vale, "Local energy markets: Paving the path toward fully transactive energy systems," *IEEE Trans. Power Syst.*, vol. 34, no. 5, pp. 4081–4088, Sep. 2019, doi: 10.1109/TPWRS.2018.2833959.

[19] A. Parisio, C. Del Vecchio, and A. Vaccaro, "A robust optimization approach to energy hub management," *Int. J. Electr. Power Energy Syst.*, vol. 42, no. 1, pp. 98–104, Nov. 2012.

[20] M. Nazari-Heris, B. Mohammadi-Ivatloo, G. B. Gharehpetian, and M. Shahidehpour, "Robust short-term scheduling of integrated heat and power microgrids," *IEEE Syst. J.*, vol. 13, no. 3, pp. 3295–3303, Sep. 2019.

[21] A. Najafi, H. Falaghi, J. Contreras, and M. Ramezani, "A stochastic bilevel model for the energy hub manager problem," *IEEE Trans. Smart Grid*, vol. 8, no. 5, pp. 2394–2404, Sep. 2017.

[22] M. Alipour, K. Zare, and H. Seyedi, "A multi-follower bilevel stochastic programming approach for energy management of combined heat and power micro-grids," *Energy*, vol. 149, pp. 135–146, Apr. 2018.

[23] F. S. Gazijahani, S. N. Ravadanegh, and J. Salehi, "Stochastic multi-objective model for optimal energy exchange optimization of networked microgrids with presence of renewable generation under risk-based strategies," *ISA Trans.*, vol. 73, pp. 100–111, Feb. 2018.

[24] J. Liu, H. Chen, W. Zhang, B. Yurkovich, and G. Rizzoni, "Energy management problems under uncertainties for grid-connected microgrids: A chance constrained programming approach," *IEEE Trans. Smart Grid*, vol. 8, no. 6, pp. 2585–2596, Nov. 2017, doi: 10.1109/TSG.2016.2531004.

[25] A. Rabiee, A. Soroudi, and A. Keane, "Information gap decision theory based OPF with HVDC connected wind farms," *IEEE Trans. Power Syst.*, vol. 30, no. 6, pp. 3396–3406, Nov. 2015, doi: 10.1109/TPWRS.2014.2377201.

[26] Z. Shi, H. Liang, S. Huang, and V. Dinavahi, "Distributionally robust chance-constrained energy management for islanded microgrids," *IEEE Trans. Smart Grid*, vol. 10, no. 2, pp. 2234–2244, Mar. 2019, doi: 10.1109/TSG.2018.2792322.

[27] Y. Liu, Y. Li, H. B. Gooi, Y. Jian, H. Xin, X. Jiang, and J. Pan, "Distributed robust energy management of a multimicrogrid system in the real-time energy market," *IEEE Trans. Sustain. Energy*, vol. 10, no. 1, pp. 396–406, Jan. 2019, doi: 10.1109/TSTE.2017.2779827.

[28] R. Lahon, C. P. Gupta, and E. Fernandez, "Optimal power scheduling of cooperative microgrids in electricity market environment," *IEEE Trans. Ind. Informat.*, vol. 15, no. 7, pp. 4152–4163, Jul. 2019, doi: 10.1109/TII.2018.2890151.

[29] B. Zhang, Q. Li, L. Wang, and W. Feng, "Robust optimization for energy transactions in multi-microgrids under uncertainty," *Appl. Energy*, vol. 217, pp. 346–360, May 2018.

[30] H. Lei, S. Huang, Y. Liu, and T. Zhang, "Robust optimization for microgrid defense resource planning and allocation against multi-period attacks," *IEEE Trans. Smart Grid*, vol. 10, no. 5, pp. 5841–5850, Sep. 2019, doi: 10.1109/TSG.2019.2892201.

WEI ZHAO (Associate Member, IEEE) received the B.S. degree, in 2001, and the Ph.D. degree from the School of Electrical and Information Engineering, Hunan University, Changsha, China, in 2010. He is currently a Senior Engineer with the Electric Power Research Institute of Guangdong Power Grid Corporation, Guangzou, China. His main research direction is advanced energy storage technology and its application in power system, electric vehicles, and energy storage operation technology.

HANBIN DIAO received the B.S. degree in electrical engineering from Hainan University, Haikou, China, in 2018. He is currently pursuing the M.S. degree with the School of Electrical and Information Engineering, Hunan University, Changsha, China. His research interest is the operation of integrated energy systems with multiple energy storage.

PEIQIANG LI received the B.S. degree from Changsha Electric Power University, Changsha, China, in 1997, and the M.S. and Ph.D. degrees from the School of Electrical and Information Engineering, Hunan University, Changsha, China, in 2004 and 2009, respectively. He is currently a Professor with the School of Electrical and Information Engineering, Hunan University, Changsha, China. His research interests include smart grid, load modeling, and electric power automation.

XIAOXIU LV received the B.S. degree from the School of Electronic and Control Engineering, Changan University, Xian, China, in 2019. She is currently pursuing the M.S. degree with the School of Electrical and Information Engineering, Hunan University, Changsha, China. Her research is integrated electric-heat system dispatch.

ERTAO LEI (Member, IEEE) received the Ph.D. degree in electrical engineering from the Huazhong University of Science and Technology, Wuhan, China, in 2017. He is currently an Engineer with the Electric Power Research Institute, Guangdong Power Grid Corporation, Guangzou, China. His research interests include reactive power control, power quality, and the application of power converters in power systems.

ZHENYU MAO received the B.S. degree in electrical engineering from Sanxia University, Yichang, China, in 2018. He is currently pursuing the M.S. degree with the School of Electrical and Information Engineering, Hunan University, Changsha, China. His research interest is power system load modeling.

WENQI XUE received the B.S. degree in automation from the Central South University of Forestry and Technology, Changsha, China, in 2018. She is currently pursuing the M.S. degree with the School of Electrical and Information Engineering, Hunan University, Changsha, China. Her research interest is electricity market transaction and software intelligentization.